Computing radiative heat transfers in greenhouses: a methodology coupling analytical and numerical approaches for view factors assessment

Samuel Sourisseau, Etienne E. Chantoiseau, Cyril Toublanc, Michel Havet

Computing radiative heat transfers in greenhouses: a methodology coupling analytical and numerical approaches for view factors assessment

S. Sourisseau[1a], E. Chantoiseau[2], C. Toublanc[1] and M. Havet[1]

[1]Oniris, Nantes Université, CNRS, GEPEA, UMR 6144, F-44000, Nantes, France; [2]Institut Agro Rennes-Angers UP EPHor Environmental Physics and Horticulture Research Unit, F-49045, Angers, France

Abstract

Soilless cultivation under heated greenhouses is a common practice for Northwestern Europe tomato producers. However, it comes with an important energy consumption that shall be more than ever addressed, especially because it still relies in a large proportion on fossil fuels. Modelling the greenhouse climate and its effects on the crop growth and yield can help to evaluate existing and innovative heating systems in relation with the associated energy consumption. Radiative heat transfers in particular shall be studied because of their magnitude compared with convection in greenhouses. However, computing view factors, which characterize how surfaces "see" each other, is complex for greenhouse where the configuration does not correspond to simplified analytical cases, with obstacles and surfaces arrangement varying with time as the crop grows.

In this work, a methodology is presented to evaluate view factors in a 1000 m^2 soilless tomato experimental greenhouse fitted with three different heating pipe networks and air ducts below the gutters. The approach uses Free and Open Source Software in conjunction with analytical solutions whenever possible to reduce computation time. The following elements are considered: floor, ducts, gutters, heating pipes, horizontal screens, roof and sidewalls. View factors that depend on the crop growth can thus be formulated to take into account the crop rows height and Leaf Area Index (LAI), from low ones (where radiative energy losses with the roof and the walls might be important to assess for year-round energy consumption studies) to mature ones. The methodology itself can not only be applied to any other greenhouse arrangement, but also more generally to any geometry where radiative transfers occur within a volume that includes obstacles.

Keywords: Radiative heat transfer, View factor, Energy efficiency, PyVista, PyViewFactor

INTRODUCTION

Heat can be transferred by conduction, convection or radiation. The first mode occurs in the matter and is driven by the internal temperature gradients: applied to process-based greenhouses climate and energy studies, conductive heat transfers are generally considered only in the soil, using for instance a one-dimension layer-by-layer discretized approach (De Zwart, 1996; Pieters et al., 1996). Convection phenomena take place between air (indoor or outdoor one) and any surface: the magnitude depend on their respective temperatures, the geometry and the flow characteristics. Correlations established in laboratories for small free-edge plates are sometimes used, but numerous formulas based on experimental studies in greenhouses are also available in the literature (Roy et al., 2002). Regarding radiative heat transfers, they result of the fact that a body above the absolute zero temperature naturally emits radiation to its environment, without involving any transfer medium. The radiative transfer rate $Q_{1\to2}$ (W) between two isothermal, diffuse and homogeneous surfaces S_1 and S_2 can be computed in its simplest form:

[a] E-mail : samuel.sourisseau@oniris-nantes.fr

$$Q_{1\to2} = \varepsilon_1 \times \varepsilon_2 \times F_{12} \times \mathrm{A}_1 \times \sigma \times (T_1^4 - T_2^4) \quad (1)$$

With ε_1 and ε_2 the emissivity of S_1 and S_2 (-), F_{12} the view factor from S_1 to S_2 (-), A_1 the area of S_1 (m^2), σ the Stefan-Boltzmann constant, T_1 and T_2 the surface temperatures of S_1 and S_2 (K). The determination of A_1 is straightforward, while a surface emissivity can either be defined from the literature, equipment datasheet or measurements. On the contrary, F_{12} depends on the surfaces geometries and orientations: it characterized the amount of radiation emitted by S_1 and directly received by S_2. Theoretically, F_{12} is computed by (Cengel, 2002):

$$F_{12} = \frac{1}{A_1} \int_{A_1} \int_{A_2} \frac{\cos\theta_1 \times \cos\theta_2}{\pi \times r^2} dA_2 dA_1 \quad (2)$$

With dA_1 and dA_2 the differential surfaces of A_1 and A_2, r the distance between these elements (m), θ_1 (θ_2) the angle between the normal to dA_1 (dA_2) and the direction $dA_1 dA_2$. F_{21} can be deduced from F_{12} considering the relationship $F_{12} \times A_1 = F_{21} \times A_2$ with A_2 the area of S_2 (m^2).

A reasonably precise calculation of radiative heat transfers, including a satisfying determination of the related view factors, is required when the radiative part is non-negligible compared to the convective one, that is generally the case in greenhouses. As far as heated ones are concerned, experimental studies focussed on hot water pipes confirm that attention has to be paid for the assessment of radiative transfers in models. For instance, according to Teitel et al. (1996) the radiation heat transfer represents between 41% to 52% of the total heat input depending on the pipes heating phase, providing calculation assumptions for the radiative part.

In the literature dedicated to protected cultivation, alternatives to Equation (2) are used to define the view factors. For infinitely large greenhouses, all the elements are modelled as horizontal homogeneous layers which are characterized by an equivalent Far Infra-Red (FIR) transmittance τ_{FIR} (-). The latter is either defined by material properties (roof), material properties and position (horizontal screens), a FIR extinction coefficient (canopy) or derived from other view factors (De Zwart, 1996). Kempkes et al. (2000) used a more complex approach by sub-dividing the crop layer into up to 9 sub-layers and by computing the view factor of a pipe to a crop layer using geometric considerations (analytical formulas). Modelling a crop arrangement in rows, Teitel and Tanny (1998) also used geometry to compute the view factors from a pipe to the other surfaces (canopy of the closest row and the opposite one, floor and roof between two rows), depending on the pipe location. Other authors applied the 1D crossed strings method, for instance to solar greenhouses (Liu et al., 2021; Zhang et al., 2020). However, the infinitely large case approach is not suitable for small greenhouses, and boundaries effects prohibit the use of 1D simplifications. Besides, elements inside the greenhouse (such as the growing gutters) may act as obstacles for the radiation between other surfaces. In such a situation, a proper computation of the view factors must be conducted.

Several numerical methods exist to compute view factors between two surfaces (Cohen and Wallace, 1993). In particular, Mazumder and Ravishankar (2012) published a general calculation procedure based on the contour method and surfaces vector representation, that can be applied to any planar polygonal surfaces. The contour integral approach consists in applying the Stokes theorem to Equation (2) and thus replacing the two surface-integrals by two contour-integrals. Recently, Bogdan et al. (2022) made use of this methodology and have implemented the free and open-source (FOSS) Python module called PyViewFactor, taking benefit of the PyVista framework (Sullivan and Kaszynski, 2019). The latter is a FOSS 3-D data visualization and post-treatment tool: it exposes all the necessary features to create, handle and display geometries as well as it facilitates mesh-based calculations. While Bodgan et al. (2022) used PyViewFactor for thermal applications in buildings and urban environment, their implementation is generic and can be applied to the protected cultivation context. In addition to the view factor calculation between any planar polygonal surface elements (cells), the module also includes functions that can be used to check if the cells are oriented in such a way

that they can actually see each other, as well as if the visibility is impaired by any obstacle using raytracing.

The present paper describes a procedure mixing analytical as well as numerical approaches using PyVista and PyViewFactor to estimate all the view factors needed to conduct year-round simulation of greenhouse energy and climate models. This methodology has been applied to an experimental heated Venlo glasshouse compartment where a soilless tomato crop was cultivated during a whole production season.

MATERIALS AND METHODS

Study case greenhouse

The case study is a 1037 m² (24 x 43.2 m) compartment of a Venlo type glasshouse located close to Nantes (France) at the Centre Technique Interprofessionnel des Fruits et Légumes (CTIFL), made of 6 spans (22° roof slope, 4 m width, 7.78 m high and 6.97 m high below the gutters). The tomato crop was laid-out in 15 rows cultivated on a rock wool medium on growing gutters, with an apex at 3.9 m from the ground for a mature crop (corresponding to a crop height from the growing gutters to the apex H_{can} of 2.8 m). Two alleyways are located at the gables (3 m large at the North, 1.2 m large at the South). Above the canopy, at the gutters height, two controlled horizontal screens (thermal and shading) were installed. The greenhouse was heated by three hot water pipe networks:

- 14 loops of "51" rails on the floor between rows (51 mm diameter)
- 15 loops of Forcas pipes in the canopy (one per row, 35 mm diameter)
- 15 loops of PE pipes (one pipe on each side of the growing gutters, 25 mm diameter)

Four 0.8 m diameter flexible perforated air-mixing ducts were installed below the growing gutters. Figure 1 illustrates how the greenhouse has been modelled.

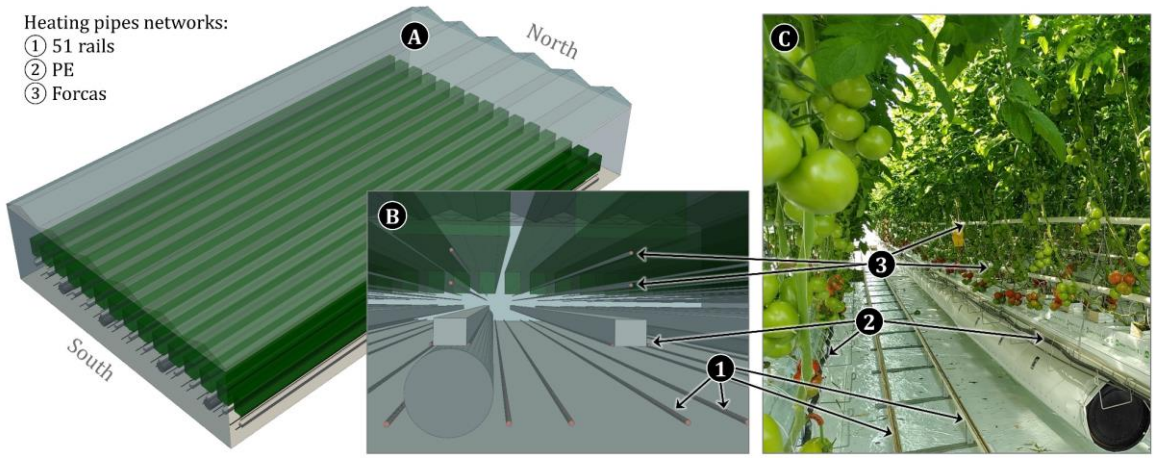

Figure 1. Study case greenhouse compartment. The global geometry (A) and its detailed view (B) correspond to 2.2 m high x 1.06 m width crop rows. C) is a picture taken while the crop was at a mature stage (2.8 m high x 1.36 m width rows).

While the greenhouse cover and equipment can boil down to simple geometries (planes, parallelepipeds and cylinders), the canopy is more complex, especially in its lower area. Although a more realistic (but significantly complex and time-consuming) geometry could be defined, in the present work opaque parallelepipedic shapes have been considered above the Forcas pipes (number 3 on Figure 1). To account for plant growth with the time, both the height and the width of the parallelepipeds were modulated according to regular plant length measurements over the whole production season. Besides, the presence of the stems, fruits and leaves at the Forcas pipes level is taken into account afterwards: the view factors obtained numerically were post-processed considering that 50% of the view factor from the Forcas pipes to any element below them (floor, growing gutters, ….) is systematically intercepted by the lower part of the canopy. Thus, for instance, the actual view factor between

the Forcas tubes and the floor $F_{Forcas \rightarrow Flr,act}$ is deduced from the value obtained with the numerical approach $F_{Forcas \rightarrow Flr,num}$ as $F_{Forcas \rightarrow Flr,act} = 0.5 \times F_{Forcas \rightarrow Flr,num}$ and the remaining part is added to $F_{Forcas \rightarrow Can,num}$.

Numerical approach

1. General procedure.

The developed script workflow is shown in Figure 2 and its implementation is available in (Sourisseau et al., 2023):

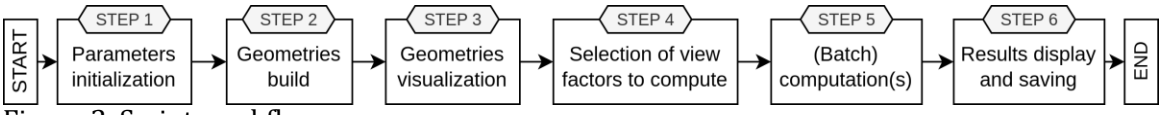

Figure 2. Script workflow

Although it is possible to import meshes from other software with PyVista, this has not been considered for the present work. On the contrary, the geometries and the meshes are built from the code using PyVista methods, based on parameter values defined at the script global level (STEP 1): greenhouse dimensions, elements sizes and position in the greenhouse, mesh type (homogeneous, heterogeneous, rectangular or triangular) and step precision, etc.

In STEP 2, the elements geometries are built. Each element has two meshes, which are exactly superimposed on each other. The first, simple, mesh is used for obstacle detection: the less cells it has, the less obstruction checks are required during the calculation process. The second one is denser and is used for the discretization of the source (S_1 in Equation (1)) and the receptor (S_2 in Equation (1)) elements from/to which a view factor is computed. Both meshes as well as all the cells normal vectors are displayed to the user at STEP 3, so that they can be carefully verified element per element.

In STEP 4, the user is asked for the selection of view factors to compute: calculations which apply to the same geometries can consequently be started in batch.

The algorithm applied in STEP 5 can be summarized as follow:

1) Distribution of the discretized cell-by-cell view factor calculations, based on the finer mesh defined on STEP 2, on all the available CPU. Parallel computing is indeed possible considering the Equation (3):

$$F_{12} = \sum_{i=1}^{N_2} F_{1i} = \sum_{i=1}^{N_2} \frac{\sum_{j=1}^{N_1} A_j \times F_{ji}}{A_1} \quad (3)$$

   With N_1 and N_2 the number of cells of the element 1 and 2 (respectively), $F_{1,i}$ the view factor from the element 1 to the i^{th} cell of element 2, A_j the area of the j^{th} cell of element 1 and F_{ji} the view factor from the j^{th} cell of element 1 to the i^{th} cell of element 2.
2) For each cell of element 2, the elementary view factors with all the cells of the element 1 were then summed. However, an elementary view factor F_{ji} is actually computed only if the following conditions, checked with PyViewFactor, are valid:
   a. The i^{th} and j^{th} cells are oriented in such a way that they can see each other.
   b. Among the possible obstacle elements cells (simpler mesh scanning), none is an obstacle to a ray drawn between the i^{th} and j^{th} cells.

Once all the cells have been treated, results are displayed and saved (STEP 6).

2. Combined use of numerical and analytical approaches.

Although the numerical approach appears simple since it "only" requires to create geometries, some drawbacks exist: defining the suitable mesh properties is not a straightforward task similarly to CFD studies, and the necessary computing time may be important. Several ways can be used to mitigate the latter issue:

- The analytical formula (Howell and Mengüç, 2011) can be kept wherever suitable for simple view factors cases with reasonable assumptions. For instance, the view factor between the screens system and the roof is obvious (two rectangular parallel plates, taking into account the cosinus of the roof slope for the roof area).

- The finer meshes cell numbers can be reduced using 1D discretization (instead of 2D) and may be made heterogeneous.
- Instead of using the whole greenhouse geometry, representative ones using fewer cells can be created for the computation of specific view factors.
- Using Equation (3), some surfaces might be split into two zones: an area where an analytical approach can be applied (simple configurations without obstacles), and the remaining one. It can be illustrated considering the case of the view factor between the floor Flr and the screens system $ScrSys$. Instead of computing it at once using the global geometry (which would require a 2D discretization dense mesh for both elements), the floor was divided into three surfaces: the cultivated one A_{cul}, and the two alleyways close to the gables at the North and South sides $A_{all,No}$ and $A_{all,So}$. The resulting view factor is formulated:

$$F_{Flr\rightarrow ScrSys} = \frac{A_{cult} \times F_{Flr,cult\rightarrow ScrSys} + A_{All,No} \times F_{All,No\rightarrow ScrSys} + A_{All,So} \times F_{All,So\rightarrow ScrSys}}{A_{cult} + A_{All,No} + A_{All,So}} \quad (4)$$

While the view factors implying the alleyways were computed using analytical formulas with reasonable assumptions, $F_{Flr,cul\rightarrow ScrSys}$ was numerically assessed considering a 1D discretization (across the greenhouse width) for the floor and the screens.

3. Time varying geometries.

Within the context of year-round greenhouse climate and energy studies, geometries may be time-dependant. For the present case, according to the applied cultivation practices, the canopy rows-based view factors have been calculated for the following estimated mean row dimensions [height x width], in m: [0 x 0], [1 x 0.6], [1.6 x 0.83], [2.2 x 1.06], [3 x 1.36] and [4 x 1.36]. Then, regression expressions linking (measured) H_{can} to the corresponding numerically assessed view factors $F_{ij,num}$ have be deduced (the last two sets of dimensions, while being over the maximum possible height (2.8 m), are used to derive suitable curves). Besides, some of the view factors that partially result from analytical formula also depend on the LAI, computed by the embedded crop yield model (Vanthoor et al., 2011).

RESULTS

Typical results with the representative geometry

The Figure 3 illustrates how the computation of a view factor is rendered after it ended, using the case between the floor cultivated area and the screens systems as an example. A representative geometry is used and since the alleyways are treated separately, a 1D discretization is sufficient.

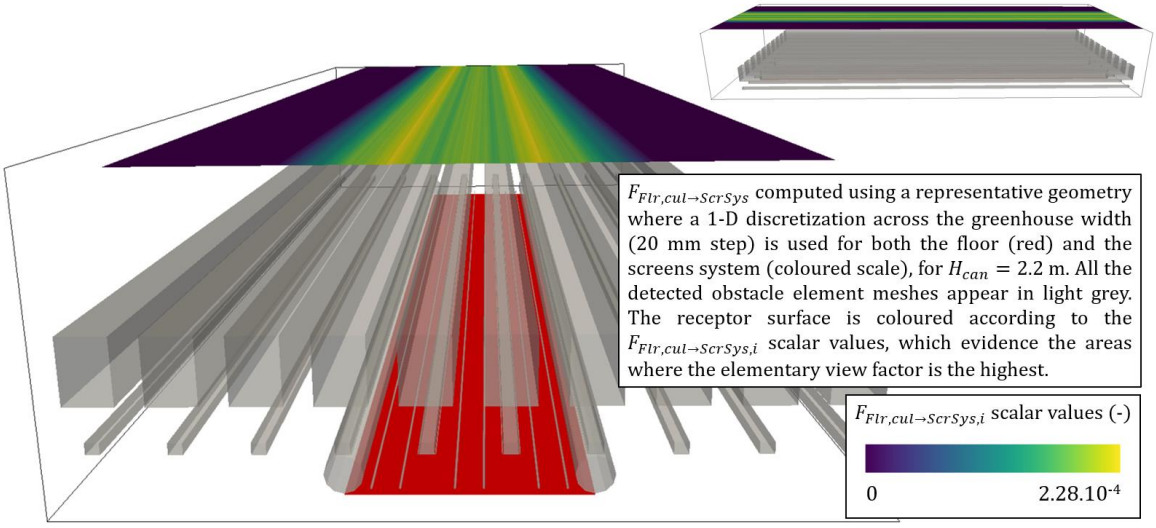

Figure 3. Displayed result for $F_{Flr,cult\rightarrow ScrSys}$, using a parametrized representative geometry.

Mesh step and computing time

For a given view factor, the required computation time highly depends on the mesh characteristics as well as on the quantity of cells of the possible obstacles. Considering the same example as Figure 3 ($F_{Flr,cult \rightarrow ScrSys}$), Figure 4 shows the effect of the discretization step across the greenhouse width for both the floor and the screens in the result accuracy. Using the value obtained with the smallest step as a reference (20 mm), the absolute difference (-) globally decreases from 0.2 m to 90 mm, but does not vary significantly from 90 mm to 20 mm.

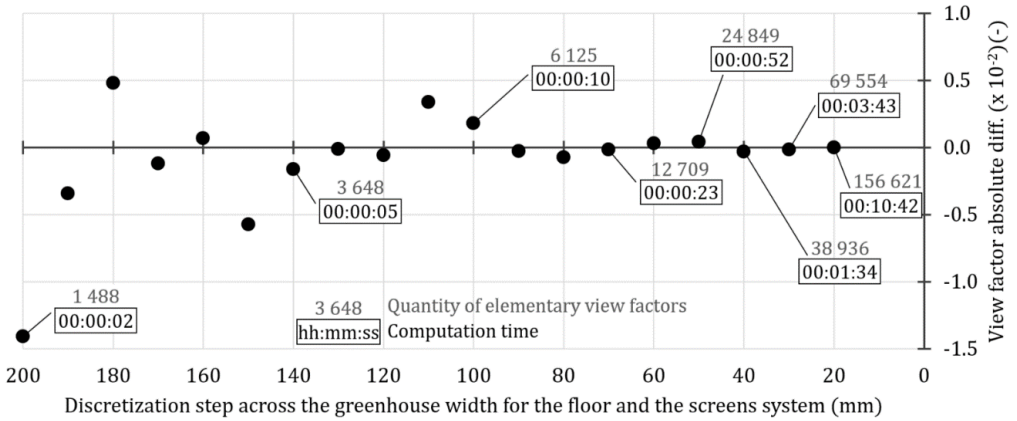

Figure 4. Absolute differences between $F_{Flr,cult \rightarrow ScrSys}$ computed with a discretization step across the greenhouse width of 20 mm for the floor and the screens, for a range of step values between 0.2 m to 20 mm.

Applied to greenhouses, where the emissivity of the surfaces, precise equipment location (such as for the flexible PE heating pipes along the growing gutters) and canopy geometry (to name but a few) are subject to uncertainty, it does not really make sense to claim an error lower than 0.01 (-) for $F_{Flr,cult \rightarrow ScrSys}$. However, since the scattering appears to be unpredictable for steps larger than 0.1 m, this value is a good compromise, in the present case, between the accuracy and calculation time.

Computations based on the same geometry but without obstacle between the floor and the screens showed that the points scattering on Figure 4 is due to the obstacle detection, not to the source and receptor surfaces discretization. Indeed, the no-obstacle absolute error is lower than $5.5.10^{-7}$(-) for all the step cases (200 → 20 mm) compared with the analytical solution of two limited rectangular parallel plates.

The indicated computation times are representative of what can be expected from the implementation in (Sourisseau et al., 2023) with a standard laptop (for the present work, a 4-cores i7-1165G7 CPU running Python 3.8.10, PyVista 0.41.1, PyViewFactor 0.0.16 and associated dependencies versions). However, possible implementation improvements have been identified but not yet investigated for the present study.

Application to a greenhouse climate and energy model

The methodology, mixing numerical approach and analytical one, has been applied to assess the view factors required to compute the thermal radiation heat transfers in a climate and energy model of the greenhouse compartment. As an example, Figure 5 (a) shows the cumulated view factors implying the screens system from the beginning of the production season (estimated canopy height H_{can} of 0.3 m and LAI of 0.5 $m^2.m^{-2}$) to the mature crop stage (2.8 m height and a LAI of 4.85 $m^2.m^{-2}$, simulated by the model). Obviously, it is expected that the view factors sum equals 1: however, the use of an analytical approach for some of the view factors as well as the scaling of the numerical results from the representative geometry to the global greenhouse one necessarily induced deviations. In the present case, the cumulated error δ remains between [+0.07:-0.02] (-) while 11 view factors are involved, and δ is mainly limited to the first weeks of the production season (the crop reached 1.3 m high 5 weeks after the planting). Starting the 11th week, the plant reached its mature high (2.8 m) for which the cumulated error appears negligible.

Once all the necessary view factors are computed (should they be constants such as for $F_{Floor \to 51\,rails}$, or functions of the crop height and LAI), the last step of the methodology consists in the normalization. For a given element, δ can be proportionally split between the view factors that have the highest expected inaccuracy due to the hypotheses that have been considered: the other view factors should not be modified. Applied to a source element X, a normalized view factor from X to the element Y is computed:

$$F_{X \to Y,norm} = F_{X \to Y} + \delta \times \frac{F_{X \to Y}}{\sum F_{X \to k}} \quad (5)$$

With k being an item in the list of all the elements on which the normalization is done (in the present case the floor, the growing gutters, the canopy and the gables (Figure 5 (b)). In dynamic models computing some of the variables on which view factors formulas depend (LAI, crop height), the normalization shall necessarily be embedded in the model itself.

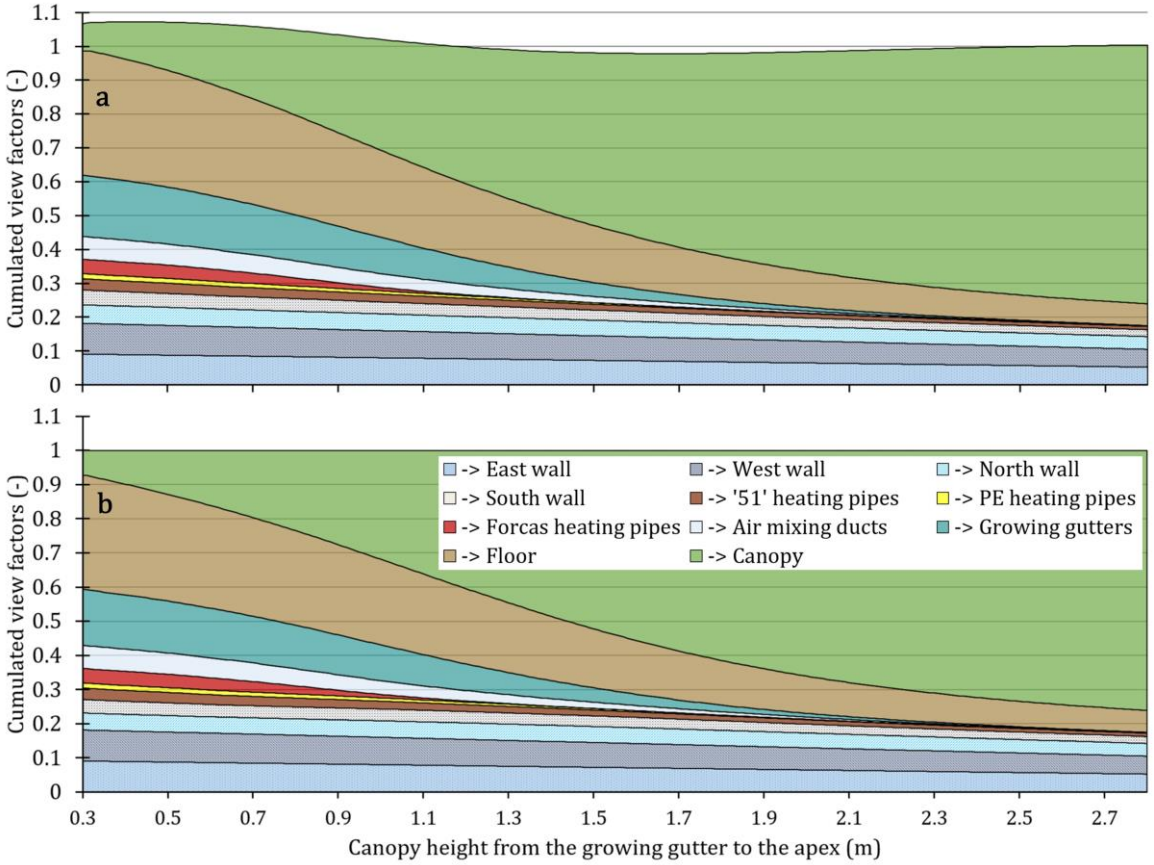

Figure 5. Cumulated view factors between the screens system and all the other elements in the greenhouse, before (a) and after (b) normalization

CONCLUSION

Whereas radiative heat transfers in greenhouses have to be taken into account in dynamic climate and energy models, the view factors assessment may be complex due to the presence of obstacles and because of the dependency on changing crop properties during the production season. A methodology mixing analytical and numerical approaches has been presented and illustrated using a 1000 m² heated compartment study case. While a full numerical approach would be the most accurate providing suitable geometries and meshes are used, the numerous view factors to compute (at different crop heights) may lead to an important calculation time on standard computer at least with proposed implementation. However, it has been shown that applying analytical formulas from the literature in conjunction with the discretization and ray-tracing based approach can provide satisfactory

view factor expressions, which may in turn be used in dynamic models. Future work would consist in implementing improvements, since moving towards more numerical resolution should alleviate the need for a normalization, The methodology will also be used to evaluate prospective technologies based on a system approach for a new fossil energy-free greenhouse concept.

ACKNOWLEDGMENTS

This study is part of SERRES+ project, funded by the regional councils of Brittany and Pays-de-Loire and supported by the Vegepolys Valley precompetitive cell. The authors would like to thank M. Bogdan for having provided PyViewFactor and for the interesting discussions and advices about view factors and obstacle detection.

Literature cited

Bogdan, M., Walther, E., Alecian, M., and Chapon, M. (2022). Calcul des facteurs de forme entre polygones – Application à la thermique urbaine et aux études de confort. (Châlons en Champagne, France), pp. 1–8.

Cengel, Y.A. (2002). Heat transfer A Practical Approach (New York: McGraw-Hill).

Cohen, M.F., and Wallace, J.R. (1993). Radiosity and realistic image synthesis.

De Zwart, H.F. (1996). Analyzing energy-saving options in greenhouse cultivation using a simulation model. Thesis. Wageningen.

Howell, J.R., and Mengüç, M.P. (2011). Radiative transfer configuration factor catalog: A listing of relations for common geometries. Journal of Quantitative Spectroscopy and Radiative Transfer *112*, 910–912. https://doi.org/10.1016/j.jqsrt.2010.10.002.

Kempkes, F.L.K., Van de Braak, N.J., and Bakker, J.C. (2000). Effect of Heating System Position on Vertical Distribution of Crop Temperature and Transpiration in Greenhouse Tomatoes. Journal of Agricultural Engineering Research *75*, 57–64. https://doi.org/10.1006/jaer.1999.0485.

Liu, R., Li, M., Guzmán, J.L., and Rodríguez, F. (2021). A fast and practical one-dimensional transient model for greenhouse temperature and humidity. Computers and Electronics in Agriculture *186*, 106186. https://doi.org/10.1016/j.compag.2021.106186.

Mazumder, S., and Ravishankar, M. (2012). General procedure for calculation of diffuse view factors between arbitrary planar polygons. International Journal of Heat and Mass Transfer *55*, 7330–7335. https://doi.org/10.1016/j.ijheatmasstransfer.2012.07.066.

Pieters, J.G., Deltour, J.M., and Debruyckere, M.J. (1996). Condensation and dynamic heat transfer in greenhouses part I: theoretical model. Int. Agric. Eng. J. *5*, 119–133. .

Roy, J.C., Boulard, T., Kittas, C., and Wang, S. (2002). PA—Precision Agriculture: Convective and Ventilation Transfers in Greenhouses, Part 1: the Greenhouse considered as a Perfectly Stirred Tank. Biosystems Engineering *83*, 1–20. https://doi.org/10.1006/bioe.2002.0107.

Sourisseau, S., Chantoiseau, E., Toublanc, C., and Havet, M. (2023). Implementation of view factors computation using a discretized approach based on PyVista and PyViewFactor, applied to a greenhouse study case with numerous obstacles. https://doi.org/10.5281/zenodo.10020604.

Sullivan, C., and Kaszynski, A. (2019). PyVista: 3D plotting and mesh analysis through a streamlined interface for the Visualization Toolkit (VTK). JOSS *4*, 1450. https://doi.org/10.21105/joss.01450.

Teitel, M., and Tanny, J. (1998). Radiative Heat Transfer from Heating Tubes in a Greenhouse. Journal of Agricultural Engineering Research *69*, 185–188. https://doi.org/10.1006/jaer.1997.0238.

Teitel, M., Shklyar, A., Segal, I., and Barak, M. (1996). Effects of Nonsteady Hot-water Greenhouse Heating on Heat Transfer and Microclimate. Journal of Agricultural Engineering Research *65*, 297–304. https://doi.org/10.1006/jaer.1996.0103.

Vanthoor, B.H.E., de Visser, P.H.B., Stanghellini, C., and van Henten, E.J. (2011). A methodology for model-based greenhouse design: Part 2, description and validation of a tomato yield model. Biosystems Engineering *110*, 378–395. https://doi.org/10.1016/j.biosystemseng.2011.08.005.

Zhang, Y., Henke, M., Li, Y., Yue, X., Xu, D., Liu, X., and Li, T. (2020). High resolution 3D simulation of light climate and thermal performance of a solar greenhouse model under tomato canopy structure. Renewable Energy *160*, 730–745. https://doi.org/10.1016/j.renene.2020.06.144.